Revista Mexicana de Astronomía y Astrofísica, **35**, 111–122 (1999)

THE MASS OF THE MILKY WAY FROM A $uvby-\beta$ SURVEY OF HIGH-VELOCITY STARS[1]

A. García Cole,[2,3] W. J. Schuster,[2] L. Parrao,[2] and E. Moreno[2]

Received 1999 March 4; accepted 1999 May 31

RESUMEN

Se han seleccionado, en el diagrama de energía de Toomre, las estrellas con velocidades más altas de nuestra campaña fotométrica $uvby-\beta$, para estimar un límite inferior para la rapidez de escape local entre 420–470 km s^{-1}. Se ha hecho un análisis cuidadoso de los errores observacionales en las distancias, movimientos propios y velocidades radiales estelares, y su propagación a las rapideces estelares totales. Se obtienen estimaciones para el tamaño de la Galaxia y su masa total, empleando esta rapidez de escape local en seis modelos de la distribución de masa Galáctica, desde modelos simples con una componente, esferoide o disco, hasta modelos más realistas con 2 y 3 componentes. Un valor conservativo para el tamaño es $\gtrsim 20-30$ kpc, y para la masa total $\gtrsim 2.0-2.5\times10^{11}\ M_\odot$. El último punto observacional en la curva de rotación Galáctica sugiere un tamaño Galáctico $\gtrsim 30-50$ kpc, y una masa total $\gtrsim 3.2-3.6\times10^{11}\ M_\odot$. Nuestra estrella más rápida, W7547, con $V_T = 509$ km s^{-1} pero $\sigma_{V_T}\sim 100$ km s^{-1}, implica los valores $\gtrsim$45 kpc y $\gtrsim 0.5\times10^{12}\ M_\odot$. Algunos de los modelos indican que hasta un 85% de la masa Galáctica puede estar en forma de materia obscura, y que alrededor del 50% de la masa total puede encontrarse en una región externa con caída rápida de la densidad del halo obscuro.

ABSTRACT

The highest-velocity stars from our $uvby-\beta$ photometric survey have been selected in the Toomre energy diagram and used to estimate a lower bound to the local escape speed, in the range 420–470 km s^{-1}. A careful analysis of the observational errors in the stellar distances, proper motions, and radial velocities, and their propagation into the total speeds has been carried out. This local escape speed plus six models for the Galactic mass distribution, from simple one-component models, spheroid or disk, to more realistic 2- and 3-component ones, give estimates for the Galactic size and total mass. A conservative measure for the size lies in the range $\gtrsim 20-30$ kpc, and for the total mass $\gtrsim 2.0-2.5\times10^{11}\ M_\odot$. The last observed point of the Galactic rotation curve would suggest a Galactic size $\gtrsim 30-50$ kpc and a total mass $\gtrsim 3.2-3.6\times10^{11}\ M_\odot$. Our fastest star, W7547, with $V_T = 509$ km s^{-1} but $\sigma_{V_T}\sim 100$ km s^{-1}, implies $\gtrsim 45$ kpc and $\gtrsim 0.5\times10^{12}\ M_\odot$. Some of these models suggest that as much as 85% of the Galactic mass may be in the form of dark matter, and that about 50% of the total mass may lie in an outer dark-halo fall-off region.

Key words: **GALAXY: FUNDAMENTAL PARAMETERS — GALAXY: KINEMATICS AND DYNAMICS**

1. INTRODUCTION

The masses of galaxies are basic for testing cosmological theories, for formulating scenarios of galactic formation, for understanding the hierarchy of galaxies and their clusters, for studying galactic and inter-

[1] Based on observations collected at the Observatorio Astronómico Nacional, San Pedro Mártir, B. C., México, and at the Danish telescopes, ESO, La Silla, Chile.

[2] Instituto de Astronomía, Universidad Nacional Autónoma de México.

[3] CCH-Naucalpan, UNAM, México.

galactic dynamics, such as that of the Local Group, for comprehending the extent and implications of dark halos and dark matter in general, and for applying gravitational lensing experiments. The mass of the Milky Way Galaxy, in which we are immersed, can be studied by various techniques, one of which is a detailed analysis of the highest-velocity stars in the solar neighborhood.

One of the first to study the shape, size, and mass of the Galaxy was Kapteyn (1922), who estimated the total number of stars in our Galaxy as 4.74×10^{10} with a mean stellar mass of 1.6 $M_\odot$, i.e., a Galactic mass of $\sim 7.6 \times 10^{10}$ $M_\odot$. However, Kapteyn overlooked the interstellar reddening, and so his estimated shape, size, mass, and center for the Galaxy are quite different from those accepted today. Much more recent works, such as those of Little & Tremaine (1987), Zaritsky et al. (1989), Leonard & Tremaine (1990), Kochanek (1996), and the review of Fich & Tremaine (1991) have discussed masses usually in the range $10^{11} - 10^{12}$ $M_\odot$. Various spectroscopic and photometric surveys have obtained similar results, such as $M_{\rm TOTAL} \gtrsim 5 \times 10^{11}$ $M_\odot$ from the work of Carney, Latham, & Laird (1988) and $M_{\rm TOTAL} \gtrsim 3.5 \times 10^{11}$ $M_\odot$ from Schuster, Parrao, & Contreras-Martínez (1993; hereafter SPC).

One of the most recent and more complete studies of the total Galactic mass is that of Kochanek (1996) who uses a Jaffe mass distribution and who applies a Bayesian statistical analysis combining all the usual methods: a) the kinematics of the Galactic satellites, including globular clusters, the Magellanic Clouds and dwarf spheroidal galaxies, b) estimates for the local escape speed using the highest-velocity nearby stars, and c) the Local Group timing method. He also invokes other restraints, such as the rotation curve of the Galactic disk and the tidal limitations placed by other Local Group members, such as M31. He obtains a Galactic mass of $(4.9 \pm 1.1) \times 10^{11}$ $M_\odot$ within 50 kpc of the Galactic center.

In this analysis, the local escape speed is estimated using the stars from our $uvby - \beta$ survey of high-velocity and metal-poor stars (Schuster & Nissen 1988, hereafter SN; SPC; and Schuster, Parrao, & García-Cole 1999, hereafter SPG). The stars with the largest speeds with respect to the Galactic center, $V_{\rm T}$, are identified in the Toomre energy diagram and are used to estimate a lower limit for the local escape speed. Not all high-velocity stars are equally reliable for this estimation; an error analysis is carried out to derive $\sigma_{V_{\rm T}}$, the standard deviation of the total speed for each star, making use of the observational errors for the photometric and astrometric distances; and for the proper motions and radial velocities. Finally several models for the Galactic mass distribution are used together with the estimated escape speed to derive values for the size and mass of the Galaxy.

Our analysis contains several advantages over other studies which have made use of the local highest-velocity stars. For example, our photometric distance calibration (Nissen & Schuster 1991; hereafter NSV) includes an evolutionary correction of the form $\delta M_{\rm v} = f \delta c_o$; we can obtain more accurate photometric distances for evolving main sequence and subgiant stars than studies using UBV photometry, for example, such as Carney et al. (1988). Nissen (1997) has shown that our photometric $M_{\rm v}$'s contain no significant systematic errors with respect to the Hipparcos values. In addition, our intrinsic-color calibration for $uvby - \beta$ photometry (Schuster & Nissen 1989a; hereafter SNII) allows us to obtain interstellar reddening measures for individual stars. In addition, our sample of approximately 1300 high-velocity and metal-poor stars has been selected differently than that of other studies, such as Carney et al. (1988); for example, with several observing runs at the European Southern Observatory our sample contains a greater percentage of southern stars. Also, a more careful and detailed error analysis than usually found in the literature has been carried out for the observed stellar speed values. Finally, a range of models for the Galactic mass distribution are used to derive the estimates for the Galactic size and mass; the results from the simplest one-component models, spheroid or disk, can be compared to the results from more realistic 2- and 3-component models; sharp-boundary models can be compared to models with a smooth density decline. Leonard & Tremaine (1990) point out that one of the principle unknowns is the mass distribution of the Galaxy exterior to the solar circle; with our several models the possible errors introduced by this uncertainty can be estimated.

However, our analysis does contain several weaknesses. Although our sample contains approximately 1300 high-velocity and metal-poor stars, as shown by Leonard & Tremaine (1990) this number is deficient by a factor of about 8 from that needed to calculate with confidence the shape of the stellar velocity distribution function near the high-velocity tail. Without this knowledge, we cannot estimate the escape speed precisely. What we do is similar to that mentioned by Fich & Tremaine (1991): our highest-velocity stars are used to estimate a lower bound for the local escape speed, and a few of these stars are excluded, in our case according to their $\sigma_{V_{\rm T}}$ errors, to account for a possible velocity-error bias, which may lead to an over-estimate for the local escape speed. In addition, no attempt is made here to include the Galactic satellites nor the Local Group timing method for estimating the Galactic mass; these techniques have been well applied in some of the references mentioned above.

2. OBSERVATIONAL DATA

The $uvby - \beta$ photometric data used in these anal-

yses come from three catalogues: that of SN which contains mostly stars from high-velocity catalogues; that of SPC, mostly high-proper-motion stars; and the SPG catalogue which is under preparation, and which contains stars from various proper-motion and abundance-study lists. The observing techniques, reduction procedures, and photometric precisions of these three catalogues are very similar and are those described in SN and SPC.

The values of $E(b-y)$ and [Fe/H] needed for the photometric distances have been derived using the intrinsic-color and metallicity calibrations of SNII. The procedures for de-reddening the photometry are given in SNII and in Schuster & Nissen (1989b). The photometric distances have been derived using the method of NSV, which includes an evolutionary correction of the form, $\delta M_V = f\,\delta c_0$, where the f coefficient is taken from Nissen, Twarog, & Crawford (1987), and δc_0 is the displacement of a star in the c_0, $(b-y)_0$ diagram from that ZAMS corresponding to the star's [Fe/H].

To carry out error analyses of the kinematic parameters, it has been assumed, as discussed in NSV, that the random distance errors vary with the evolutionary correction, δM_V. For $\delta M_V \leq 0\overset{m}{.}25$, the distance error has been taken as 10%; for $0\overset{m}{.}25 < \delta M_V \leq 0\overset{m}{.}75$, 12.5%; for $0\overset{m}{.}75 < \delta M_V \leq 1\overset{m}{.}50$, 15%; and for $\delta M_V > 1\overset{m}{.}50$, 25%. One of our fastest stars, HD 229274, is very evolved and has $\delta M_V = 6.383$; the above scheme provides only a lower limit to its distance uncertainty.

For the stars of the three photometric catalogues, a preliminary kinematic analysis was carried out as in § 8, Table 7, and Figure 4 of SPC. For this preliminary work the stellar radial velocities were generally taken from the sources listed in NSV, such as Abt & Biggs (1972), Fouts & Sandage (1986), Carney & Latham (1987), Norris & Ryan (1989), and Ryan & Norris (1991). Once the stars with the largest speeds with respect to the center of the Galaxy had been identified, final radial velocity values were selected from more recent and more precise sources, whenever possible, such as from Turon et al. (1992) and from Carney et al. (1994). Generally, these final values were within 5 km s^{-1} of the preliminary values. The mean standard deviations of the final radial velocities are generally less than $\pm$ 1.0 km s^{-1}, and less than or equal to $\pm$ 7.0 km s^{-1} for all the more rapid stars for which error estimates are available.

The preliminary proper motions were taken from many sources; those listed in NSV, such as Eggen (1964), the SAO catalogue (Ochsenbein 1979), Giclas, Burnham, & Thomas (1971; 1978), and Luyten (1957; 1961, hereafter LTT). Whenever possible the final proper motions were taken from The Hipparcos Catalogue (ESA 1997), and when not, from Luyten (1979; 1980, hereafter NLTT), LTT, and Lowell proper-motion surveys. Typical errors in μ_α and μ_δ fall in the range $\pm 0.001''$ yr^{-1} to $\pm$ 0.006$''$ yr^{-1} for the values from The Hipparcos Catalogue, and in the range $\pm$ 0.020$''$ yr^{-1} to $\pm$ 0.025$''$ yr^{-1} for the other sources.

Representative errors of the stars' total space velocities lie in the range $\pm$ 20 to $\pm$ 70 km s^{-1}, as seen below in Tables 2 and 3. For most of these high-velocity stars, the largest contribution to this error arises from the uncertainty of the distance determination (see Table 3 below). For the three closest stars, HD 134439, HD 134440, and $-$36:12201, the Hipparcos parallaxes provide stellar distances with similar or better precision and accuracy than the photometric method. For these three stars, the kinematics and errors have been calculated using both the photometric and parallactic distances. In Tables 1 to 3 an "H" suffix to the star name indicates that the parallactic (Hipparcos) distance has been used.

3. GALACTIC VELOCITIES

The values and errors of the Galactic space velocities, (U, V, W), have been calculated according to the equations and formulism of Johnson & Soderblom (1987) using a computer program graciously loaned to us by C. Allen. In Table 1 are given the coordinates and kinematic data used to derive the space velocities and their errors for the 15 highest-velocity stars from the three photometric catalogues. The last four columns of this table give the error estimates for the two proper-motion components, the radial velocities, and the photometric and parallactic distances, respectively. When these error estimates have not been given in the literature, errors of $\pm$ 0.025$''$ yr^{-1} have been assumed for the two proper-motion components and $\pm$ 7.0 km s^{-1} for the radial velocity determinations; these estimates correspond to the larger errors found in the proper-motion catalogues mentioned above, such as the NLTT, LTT, and Lowell proper-motion survey (Giclas et al. 1971; 1978), and in the radial-velocity studies of Fouts & Sandage (1986) and Norris & Ryan (1989).

To select these highest-velocity stars, the preliminary Toomre energy diagram of Figure 1 has been used. $[U'^2 + W'^2]^{1/2}$ is plotted versus V', where the space velocities (U', V', W') are those with respect to the Local Standard of Rest. In Figure 1, the concentric circles are centered on the point ($-$220, 0) km s^{-1}, represent circles of constant kinetic energy in the Galaxy, and can be used to select the most rapid stars with respect to the Galactic center. These most rapid stars provide us with a lower limit for the local Galactic escape speed, assuming that all such stars are in fact bound to the Galaxy (see Leonard & Tremaine 1990).

In Table 2 are shown the 15 highest-velocity stars from our sample with their calculated Galactic space velocities and errors. Columns 2 and 3 contain the

TABLE 1

INPUT KINEMATIC DATA AND ESTIMATED ERRORS

Name	R.A. (1950) (h m s)	Dec. (° ′ ″)	μ_α (″ yr^{-1})	μ_δ (″ yr^{-1})	Radial Vel. (km s^{-1})	Dist. (pc)	Estimated Errors μ_α (″ yr^{-1})	Estimated Errors μ_δ (″ yr^{-1})	Estimated Errors Radial Vel. (km s^{-1})	Estimated Errors Dist. (pc)
G033–031	00 58 44.00	+14 58 54	+0.299	+0.034	+255.6	154.0	0.025	0.025	0.22	19.0
G095–011	03 06 56.00	+34 39 36	+0.282	−0.007	+205.7	251.0	0.025	0.025	0.30	31.0
W3314	05 26 53.50	−29 55 19	+0.375	−0.273	+542.8	122.0	0.002	0.003	7.00	12.0
G041–041	09 26 34.70	+08 51 31	+0.199	−0.308	+266.1	292.0	0.003	0.002	0.24	44.0
W7547	12 29 49.90	−39 49 23	−0.349	+0.079	− 40.0	328.0	0.025	0.025	7.00	49.0
G064–012	13 37 29.62	+00 12 57	−0.230	−0.080	+441.9	286.0	0.002	0.002	0.35	43.0
G201–005	14 34 36.00	+55 46 12	+0.130	−0.280	− 35.6	235.0	0.025	0.025	0.21	29.0
HD 134440	15 07 28.33	−16 13 29	−1.001	−3.543	+311.5	29.0	0.001	0.001	0.20	3.0
HD 134440H	15 07 28.33	−16 13 29	−1.001	−3.543	+311.5	29.7	0.001	0.001	0.20	1.5
HD 134439	15 07 28.48	−16 08 27	−0.999	−3.543	+310.6	33.0	0.001	0.001	0.17	4.0
HD 134439H	15 07 28.48	−16 08 27	−0.999	−3.543	+310.6	29.3	0.001	0.001	0.17	1.2
G015–013	15 10 05.00	+06 13 24	−0.450	−0.659	+219.0	134.0	0.006	0.003	0.24	17.0
−36:12201	18 02 33.90	−36 35 42	−0.277	−0.227	+364.0	86.0	0.002	0.001	7.00	13.0
−36:12201H	18 02 33.90	−36 35 42	−0.277	−0.227	+364.0	64.7	0.002	0.001	7.00	8.8
811–024	19 04 38.00	−19 41 36	−0.074	−0.241	−152.0	601.0	0.025	0.025	7.00	150.0
HD 229274	20 22 50.38	+41 20 21	−0.096	−0.135	−162.2	619.0	0.001	0.001	7.00	186.0
G026–012	21 31 02.00	+00 10 18	+0.244	−0.032	−239.3	338.0	0.006	0.003	0.28	51.0
G126–063	22 09 12.00	+17 48 12	+0.342	−0.026	−168.7	273.0	0.025	0.025	0.20	41.0

Galactic latitudes and longitudes, columns 4 to 6 the space velocities with respect to the Local Standard of Rest, and columns 7 to 9 the estimated standard deviations of these three velocities, respectively. These stars have been ordered according to their total speeds with respect to the Galactic center, which are given in the last two columns together with their estimated errors. It can be easily seen that not all these rapid stars are equally appropriate for estimating the local escape speed (see Leonard & Tremaine 1990). For example, three of the fastest stars, W7547, 811–024, and HD 229274, have large errors, ± 99.9 km s^{-1}, ± 205.7 km s^{-1}, and ± 145.8 km s^{-1}, respectively, for their total speeds. Similar to SPC, we conclude from Table 2 that a reliable lower limit for the local escape speed lies in the range 420–470 km s^{-1}, based on such stars such as HD 134439/40, HD 134439H/40H, G064–012, and G033–031.

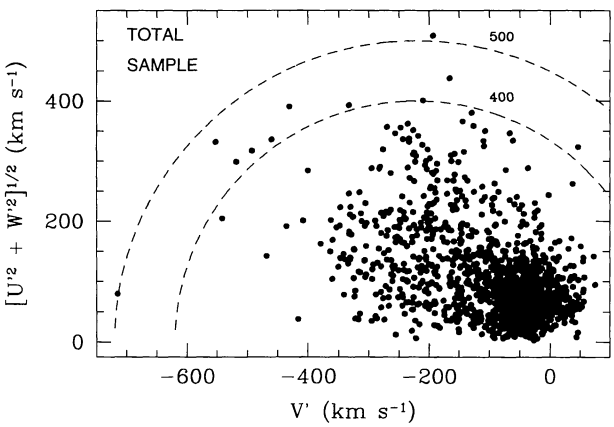

Fig. 1. The preliminary Toomre energy diagram, $[U'^2 + W'^2]^{\frac{1}{2}}$ versus V', for our total sample of high-velocity stars. The two semicircles represent speeds with respect to the Galactic center of 400 and 500 km s^{-1}.

In Table 3 are repeated the 15 highest-velocity stars with their total space speeds and corresponding errors; also shown are the components of this error due to the observational uncertainties in the stellar distances, proper motions, and radial velocities. As mentioned above, the largest contribution to this total-speed error generally comes from the stellar distance. For stars not measured by Hipparcos, the proper-motion error also sometimes makes a significant contribution (the stars W7547, 811–024, G033–031, G126–063, G201–005, and G095–011).

4. MODELS FOR THE GALACTIC MASS DISTRIBUTION

In this section six models for the Galactic mass distribution are given to which our observational data are applied (next section) to estimate the total

TABLE 2

GALACTIC SPACE VELOCITIES AND ESTIMATED ERRORS[a]

Name	Galactic Lat. (degrees)	Galactic Long. (degrees)	U'	V'	W'	$\sigma_{U'}$	$\sigma_{V'}$	$\sigma_{W'}$	V_T	σ_{V_T}
W7547	22.6	299.0	504.3	−193.5	65.0	82.0	43.0	37.6	509.1	99.9
811–024	−12.2	17.0	− 55.7	−715.0	− 56.9	53.7	184.5	73.7	501.4	205.7
HD 134439	35.0	344.8	−322.1	−551.3	− 92.9	8.1	60.5	33.8	471.3	69.8
HD 229274	2.2	79.4	−456.4	−233.3	1.2	143.1	27.6	2.5	456.6	145.8
G064–012	60.4	328.2	− 8.4	−373.0	400.5	28.2	41.1	1.8	428.8	49.9
HD 134440H	35.0	344.7	−315.5	−502.0	− 65.0	3.0	22.7	12.7	428.1	26.2
HD 134439H	35.0	344.8	−314.6	−495.3	− 61.6	2.4	18.2	10.1	422.6	20.9
HD 134440	35.0	344.7	−314.1	−491.4	− 59.0	6.0	45.4	25.4	419.3	52.4
G033–031	−47.6	126.5	282.9	46.7	−156.0	28.8	20.2	12.7	418.9	37.4
G041–041	38.9	224.2	−232.5	−473.6	206.5	56.0	51.9	5.8	401.3	76.6
G126–063	−30.5	77.8	357.4	−219.6	−180.8	59.7	22.3	49.7	400.6	80.9
G026–012	−35.1	54.6	365.5	−206.7	−142.3	40.3	10.0	44.0	392.4	60.5
W3314	−30.0	233.5	147.9	−555.3	−121.3	12.6	19.6	14.4	386.0	27.4
−36 12201H	− 7.5	355.5	−367.1	−115.5	0.7	6.9	13.9	5.6	381.7	16.5
G201–005	55.9	96.5	−343.9	− 66.8	45.4	49.5	24.4	17.7	379.2	57.9
G015–013	50.4	7.2	−226.8	−468.3	164.2	10.2	63.6	2.6	374.3	64.5
−36 12201	− 7.5	355.5	−366.2	−149.1	14.1	6.9	20.5	8.3	373.3	23.2
G095–011	−19.9	152.7	346.1	−125.4	99.7	28.0	39.0	34.4	372.4	59.1

[a] In km s^{-1}.

TABLE 3

TOTAL SPEEDS, ESTIMATED ERRORS, AND THE COMPONENTS OF THESE ERRORS[a]

Name	V_T	σ_{V_T}	Error Stellar Distance	Error Proper Motion	Error Radial Velocity
W7547	509.1	99.9	83.1	55.0	7.0
811–024	501.4	205.7	179.3	100.7	7.0
HD 134439	471.3	69.8	69.8	0.2	0.2
HD 229274	456.6	145.8	145.5	3.5	7.0
G064–012	428.8	49.9	49.7	4.2	0.3
HD 134440H	428.1	26.2	26.2	0.3	0.2
HD 134439H	422.6	20.9	20.9	0.2	0.2
HD 134440	419.3	52.4	52.4	0.3	0.2
G033–031	418.9	37.4	27.1	25.8	0.2
G041–041	401.3	76.6	76.4	5.3	0.2
G126–063	400.6	80.9	66.7	45.8	0.2
G026–012	392.4	60.5	59.5	11.2	0.3
W3314	386.0	27.4	26.4	1.8	7.0
−36 12201H	381.7	16.5	14.9	0.8	7.0
G201–005	379.2	57.9	42.4	39.4	0.2
G015–013	374.3	64.5	64.3	4.4	0.2
−36 12201	373.3	23.2	22.1	1.1	7.0
G095–011	372.4	59.1	41.5	42.1	0.3

[a] In km s^{-1}.

mass of our Galaxy and its outer boundary. These models include the popular spherical model (Sandage & Fouts 1987; Carney et al. 1988; Cudworth 1990, SPC), and the detailed Galactic model of Allen & Santillán (1991) with a sharp boundary, and also with a smooth decline for its external density. Also included is a disk model, which has not been considered in discussions about an estimate of the Galactic mass, yet has been available since the work of Mestel (1963). Of the two remaining models, one is a combination of the spherical and disk models, and the other is obtained from a mass distribution used to fit rotation curves of plane galaxies (Pişmiş & Moreno 1999).

Simple Galactic Models

a) Spherical Model

The well known equations for this model are the following (in all models the units are such that $G = 1$): the mass density is $\rho(r) = \rho_o/r^2$, so the rotation speed at all radii is a constant Θ_o. To make the total mass finite we take a boundary at $r = r_{max}$, so the total mass is

$$M_{sph} = \Theta_o^2 r_{max} \ . \qquad (1)$$

The gravitational potential (per unit mass) $\Phi(r)$ for $r < r_{max}$ is given by $\Phi(r) = -\Theta_o^2 [1 + ln(r_{max}/r)]$. The escape speed, $v_e(r)$ for $r < r_{max}$, is then given by

$$v_e^2(r) = 2\Theta_o^2 \left(1 + ln \frac{r_{max}}{r}\right) \ . \qquad (2)$$

r_{max} is obtained from this equation (2) given the value Θ_o and evaluating at the solar position with the observed lower limit for $v_e^2(r)$ (assuming that the Sun lies inside r_{max}; this is checked with the value obtained for r_{max}); the total mass then follows from equation (1).

b) Disk Model

Mestel (1963) shows that a disk with radius R_{max} and surface density given by

$$\sigma(R) = \frac{\Theta_o^2}{2\pi R} \left(1 - \frac{2}{\pi} \arcsin \frac{R}{R_{max}}\right) \ ; \quad R \leq R_{max} \qquad (3)$$

gives a flat rotation curve $\Theta(R) = \Theta_o$. The total mass of the disk is easily found from equation (3)

$$M_D = \frac{2\Theta_o^2 R_{max}}{\pi} \ . \qquad (4)$$

The gravitational potential for $R \leq R_{max}$ is $\Phi(R) = -\Theta_o^2 ln(2R_{max}/R)$. Then the escape speed $v_e(R)$ for $R \leq R_{max}$ is

$$v_e^2(R) = 2\Theta_o^2 ln \left[\frac{2R_{max}}{R}\right] \qquad (5)$$

As in the spherical model, R_{max} is found evaluating equation (5) at the solar position, and then the total mass from equation (4). Two simple relations follow from equations (1), (2), (4), and (5) applied to the same values of R_o, Θ_o, and $v_e(R_o)$ (R_o, the Sun's Galactocentric distance): $M_{sph}/M_D = \pi/e \approx 1.1557$, $r_{max}/R_{max} = 2/e \approx 0.7357$; i.e., the spherical model gives a slightly greater total mass but with a significantly less dimension for its outer boundary, compared with the values obtained in the disk model.

c) Combination of Spherical and Disk Models

A more realistic simple model for our Galaxy is a combination of the previous two models. The spherical and disk components are taken having the same radial dimension R^*_{max}, and giving a total constant rotation speed Θ_o for $R \leq R^*_{max}$. Then with $\Theta_o^2 = \Theta_{sph}^2 + \Theta_D^2$ and $\Theta_{sph}^2 = \mu\Theta_o^2$, $\mu \leq 1$, the total mass is (using eqs. 1 and 4)

$$M_{sph,D} = \Theta_{sph}^2 R^*_{max} + \frac{2\Theta_D^2 R^*_{max}}{\pi} = \Theta_o^2 R^*_{max} \left[\frac{2}{\pi}(1-\mu) + \mu\right] \ . \qquad (6)$$

The expression for $\Phi(R)$, $R \leq R^*_{max}$, is now

$$\Phi(R) = -\Theta_o^2 ln \left[2\left(\frac{e}{2}\right)^{\mu} \frac{R^*_{max}}{R}\right] \ ,$$

from which the escape speed is

$$v_e^2(R) = 2\Theta_o^2 ln \left[2\left(\frac{e}{2}\right)^{\mu} \frac{R^*_{max}}{R}\right] \ . \qquad (7)$$

Taking $\mu = 1, 0$ in equations (6) and (7) we recover the limiting cases equations (1), (2) (spherical) and (4), (5) (disk), respectively. For other values of μ and with a fixed set (R_o, Θ_o, $v_e(R_o)$), it is readily shown that R^*_{max} and $M_{sph,D}$ obtained from equations (7) and (6) satisfy $r_{max} < R^*_{max} < R_{max}$ and $M_D < M_{sph,D} < M_{sph}$.

Three-Component Galactic Models

d) Approximate 3-Component Model

The three previous models give exactly a flat rotation curve in the plane of symmetry within the maximum radial dimension. We now consider a three-component model which approximately reproduces the greater detail shown by the actual rotation curve in our Galaxy, and also the local (solar neighborhood) properties: Oort's constants, the mass density, and the acceleration in the z-direction. This approximate simple model is obtained from the mass dis-

tribution considered by Pişmiş & Moreno (1999) to fit rotation curves and surface brightnesses in plane galaxies. The model has been found to work in about 50% of the sixty-two spiral galaxies listed by Rubin et al. (1985), and has a very simple density law for each component. For the disk component it consists of a Schmidt type oblate spheroid with similar strata and density of the form $\rho_{\rm D}(a) = q/a + pa$, $a \leq a_{\rm D}$ (see Schmidt 1956). The other two components are spherical, one representing the stellar bulge and halo, and the other the dark halo. Both components have the polynomial density

$$\begin{aligned} \rho(a) &= c_1 a^n + c_2 a^m, \quad a \leq a_{\rm t} \ , \\ \rho(a) &= c_3 a^s, \qquad\qquad a \geq a_{\rm t} \ . \end{aligned} \tag{8}$$

where c_1, c_2, and c_3 are constants; (n, m) can have the values $(-1, 0)$, $(-1, 1)$, or $(0, 1)$, and $s = -2$, or -5. The stellar bulge-halo takes any one of the three pairs (n, m) with $s = -5$; the dark halo is represented with $(n, m) = (-1, 1)$, $s = -2$. The distance $a_{\rm t}$, different for each component, is a transition distance where the density changes its functionality. The density and its derivative are continuous at $a_{\rm t}$, and so only one constant, say c_3, is needed from c_1, c_2, c_3. Using these three components, we have made a numerical search to find the best fit to the Galactic rotation curve and local properties. Our best fit is shown in Figure 2, which presents the fit to the rotation curve; the observational data is taken from Allen & Santillán (1991).

Other properties of the fit are the following: eccentricity, radius, and mass of the oblate spheroid: $e = 0.9987$, $a_{\rm D} = 10.07$ kpc, $M_{\rm D} = 3.93 \times 10^{10}\ M_\odot$; transition distance in the dark halo and its mass within this radius: $(a_{\rm t})_{\rm DH} = 7.54$ kpc, and $M_{\rm DH}((a_{\rm t})_{\rm DH}) = 3.16 \times 10^{10}\ M_\odot$; Oort's constants and local mass density: $A = 15.57$ km s^{-1} kpc^{-1}, $B = -14.24$ km s^{-1} kpc^{-1}, and $\rho = 0.13\ M_\odot$ pc^{-3};

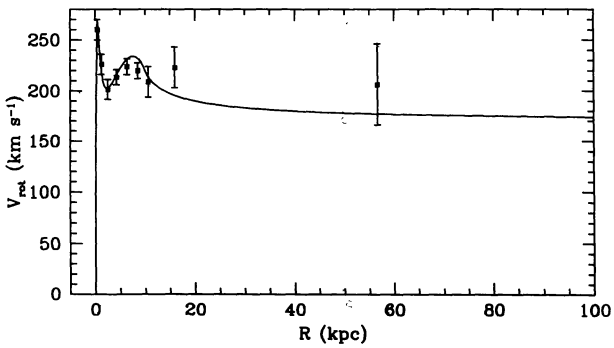

Fig. 2. Model (d); our best fit (continuous line) to rotational data in our Galaxy (points), taken from Allen & Santillán (1991).

Sun's Galactocentric distance: $R_{\rm o} = 7.85$ kpc. The three possible values for (n, m) in the stellar bulge-halo give almost exactly the same fit. Then as a representative case, with $(n, m) = (-1, 1)$ the transition distance in the stellar bulge-halo is $(a_{\rm t})_{\rm SH} = 0.47$ kpc and its total mass is $M_{\rm SH} = 1.11 \times 10^{10}\ M_\odot$. The total mass in the dark halo up to a distance $a_{\rm max} (\geq (a_{\rm t})_{\rm DH})$ is given by

$$M_{\rm DH}(a_{\rm max}) = \frac{1}{5} M_{\rm DH}((a_{\rm t})_{\rm DH}) \left[\frac{8 a_{\rm max}}{(a_{\rm t})_{\rm DH}} - 3 \right] \ . \tag{9}$$

The gravitational potential at the solar position $R_{\rm o} = 7.85$ kpc (which is a function of $a_{\rm max}$, the outer boundary of the dark halo) can easily be found, and also its relation with the local escape speed $v_{\rm e}$. From this relation we obtain $a_{\rm max}$ in terms of $v_{\rm e}$ in the final form

$$a_{\rm max} = 7.85 \exp \left\{ 0.12 \left[0.029 \left(\frac{1}{2} v_{\rm e}^2 - 310.104 \right) + 3 \right] - 1 \right\} \ {\rm kpc} \ . \tag{10}$$

In this equation $v_{\rm e}$ is given in units of 10 km s^{-1}. Introducing $v_{\rm e}$ in equation (10) we get $a_{\rm max}$, and then $M_{\rm DH}(a_{\rm max})$ from equation (9). The total mass is $M = M_{\rm D} + M_{\rm SH} + M_{\rm DH}(a_{\rm max})$.

The main application of the present model consists in the following extension: instead of taking an abrupt boundary in the dark halo, we consider that at a distance $a_{\rm ext} > (a_{\rm t})_{\rm DH}$ this halo has again a transition in its density, making its total mass finite. This external region for $a \geq a_{\rm ext}$ will not affect the properties of the fit for $a \leq a_{\rm ext}$, but the gravitational potential at the solar position will change.

A density function for $a \geq a_{\rm ext}$ which falls faster than a^{-2} and gives a finite total mass for the dark halo, having at the same time a smooth transition (the function and its first derivative being continuous at $a_{\rm ext}$) is

$$\rho(a) = \frac{k c_3}{(k-2) a_{\rm ext}^2 \left[1 + \frac{2}{k-2} \left(\frac{a}{a_{\rm ext}} \right)^k \right]} \ ; \qquad a \geq a_{\rm ext} \tag{11}$$

with $k \geq 4$.

The situation with this external region is now the following: the gravitational potential at the solar position is a function of $a_{\rm ext}$ for a given $k \geq 4$, and we find

$$a_{\rm ext} = a_{\rm max} e^{-\gamma} \ , \tag{12}$$

with $a_{\rm max}$ given by equation (10) and γ a positive constant depending on the value of k. Some values for γ are: $k = 4$, $\gamma = \pi/4 \simeq 0.7854$; $k = 5$, $\gamma \simeq$

0.5779; $k = 6$, $\gamma \simeq 0.4664$. The total (finite) mass of the dark halo is now

$$M_{\rm DH} = \frac{1}{5} M_{\rm DH}((a_{\rm t})_{\rm DH}) \left[2 \left(\frac{a_{\rm ext}}{(a_{\rm t})_{\rm DH}} \right) \left(4 + \frac{\lambda}{\pi} \right) - 3 \right] , \quad (13)$$

with λ also being a constant depending on the value of k: $k = 4$, $\lambda \simeq 21.7894$; $k = 5$, $\lambda \simeq 11.9236$; $k = 6$, $\lambda \simeq 8.4887$. In the limit $k \to \infty$, i.e., abrupt boundary in the dark halo, γ and λ must tend to zero, and so eqs. (13), (12) give eqs. (9), (10). With $v_{\rm e}$ and a given k (we take $k = 4, 5, 6$), $a_{\rm ext}$ is found from equation (12) and then $M_{\rm DH}$ from equation (13). The total mass is $M = M_{\rm D} + M_{\rm SH} + M_{\rm DH}$.

e) Galactic Model of Allen & Santillán (1991); Sharp Boundary

The Galactic model of Allen & Santillán (1991) reproduces very satisfactorily the rotation curve and local properties of our Galaxy. It is a three-component model: it has an infinite disk, an infinite spherical component to represent the Galactic bulge, and a spherical dark halo with a finite boundary. In passing, let us state the similarities between this most convenient model and the approximate one given by model **(d)**: both models have three components; their spherical halos representing the bulge-halo both have an external r^{-5} dependence starting from almost the same distance; the dark halos have the same r-dependence in the inner and outer regions, r^{-1} and r^{-2}, respectively. Their main difference is that model **(d)** has a finite disk component, and in the model of Allen & Santillán the disk is infinite.

With equations given by Allen & Santillán (1991), the gravitational potential at the solar position ($R_{\rm o} = 8.5$ kpc) can readily be found, being a function of $a_{\rm max}$: the outer boundary of the dark halo. Connecting this potential with the local escape speed $v_{\rm e}$, we arrive at the following expression relating $a_{\rm max}$ and $v_{\rm e}$

$$-\frac{1.02}{1 + u_{\rm max}} + ln(1 + u_{\rm max}) \approx 2.652 \times 10^{-3} \left[\frac{1}{2} v_{\rm e}^2 - 618.112 \right] , \quad (14)$$

where $u_{\rm max} = (a_{\rm max}/12 \text{ kpc})^{1.02}$ and $v_{\rm e}$ in units of 10 km s^{-1}. Once $u_{\rm max}$ (and then $a_{\rm max}$) is found from equation (14), the mass of the dark halo, $M_{\rm DH}(a_{\rm max})$, up to the distance $a_{\rm max}$ is given in units of $2.32 \times 10^7\ M_\odot$ by

$$M_{\rm DH}(a_{\rm max}) = \frac{4615 (u_{\rm max})^{2.02/1.02}}{1 + u_{\rm max}} . \quad (15)$$

The total mass is then

$$\frac{M}{2.32 \times 10^7\ M_\odot} = 4296 + M_{\rm DH}(a_{\rm max}) . \quad (16)$$

f) Galactic Model of Allen & Santillán (1991); Smooth Density Decline

As in the extension considered in model **(d)**, a density function for the external region $a \geq a_{\rm ext}$ has been considered for the Galactic model of Allen & Santillán (1991) with the following form

$$\rho(a) = \frac{Q_1}{Q_2 + \left(\frac{a}{a_{\rm ext}} \right)^k} \quad ; \ a \geq a_{\rm ext}, \ k \geq 4 . \quad (17)$$

The expressions for the coefficients Q_1, Q_2, $a_{\rm ext}$, the total (finite) mass of the dark halo, and the total Galactic mass are easily obtained.

TABLE 4

DERIVED SIZES AND MASSES IN MODELS (a)-(c) AND (e)

Star	Distances[a] $r_{\rm max}$ (a)	$R_{\rm max}$ (b)	$R^*_{\rm max}$ (c)	$a_{\rm max}$ (e)	Masses[b] (a)	(b)	(c)	(e)
W7547	45.49	61.83	48.37	69.34	5.11	4.42	5.04	6.30
HD 134439	31.02	42.16	34.12	42.21	3.48	3.02	3.40	3.95
G064–012	20.90	28.40	24.14	24.74	2.35	2.03	2.25	2.49
HD 134440H	20.77	28.23	24.06	24.53	2.33	2.02	2.23	2.47
HD 134439H	19.79	26.89	23.07	22.92	2.22	1.93	2.12	2.34
HD 134440	19.23	26.13	22.48	22.00	2.16	1.87	2.06	2.27

[a] In kpc.

[b] In units of $10^{11}\ M_\odot$.

5. RESULTS

Tables 4, 5, and 6 give the derived sizes and masses for the models developed in § 4, corresponding to our six fastest stars with the lesser observational errors. Table 4 presents the results for the sharp boundary models **(a)** spherical, **(b)** disk, **(c)** combination of spherical plus disk, and **(e)** Allen & Santillán (1991); while Table 5, **(d)** the approximate three-component model, and Table 6, **(f)** the extension of the Galactic model of Allen & Santillán (1991).

Calculations are carried out for the star W7547 only because it is our fastest, but with an error of $\sigma_{V_T} \approx 100$ km s^{-1} its results are not too reliable. Better, more conservative, estimates for the mass and size of the Galaxy are obtained from the stars HD 134439/40 and G064–012.

In model **(c)**, the combination of spherical and disk models, μ is estimated as follows: we consider the Galactic model of Allen & Santillán (1991), and for a given star we take the ratio $\eta = M_{\rm DH}(a_{\rm max})/M_{\rm DISK}$, with $M_{\rm DH}(a_{\rm max})$ given by equation (15) and $M_{\rm DISK} = 3690$, the mass of the disk (in the same units as eq. 15) in the model of Allen & Santillán (1991). Then it is easy to show that $1/\mu = 1 + \pi/2\eta$, and this is used in eqs. (7) and (6) to obtain the distances and masses listed in Table 4 for this model **(c)**.

Table 5 gives the derived distances $a_{\rm ext}$ (eq. 12) and corresponding total masses in model **(d)**. The first to fourth line in each case corresponds to $k = 4$, 5, 6, and $k \to \infty$, respectively (this last limit gives eq. (10) and its associated total mass). Table 6 gives the values for $a_{\rm ext}$ and the total mass in model **(f)**, with $k = 4$, 5, 6; the corresponding values with $k \to \infty$ are those given in Table 4 for model **(e)**.

TABLE 5

DERIVED DISTANCES[a] AND MASSES[b] IN MODEL (**d**)

	W7547	HD 134439	G064–012	HD 134440H	HD 134439H	HD 134440	k
	57.08	30.07	15.52	15.36	14.17	13.50	4
$a_{\rm ext}$	70.24	37.00	19.10	18.90	17.43	16.62	5
	78.53	41.38	21.36	21.13	19.49	18.58	6
	125.19	65.96	34.04	33.69	31.07	29.62	∞
	10.80	5.83	3.16	3.13	2.91	2.79	4
M	9.50	5.15	2.81	2.78	2.59	2.49	5
	9.14	4.97	2.71	2.69	2.51	2.40	6
	8.71	4.74	2.60	2.57	2.40	2.30	∞

[a] In kpc.
[b] In units of 10^{11} $M_\odot$.

TABLE 6

DERIVED DISTANCES[a] AND MASSES[b] IN MODEL (**f**)

	W7547	HD 134439	G064–012	HD 134440H	HD 134439H	HD 134440	k
	31.48	19.13	11.19	11.10	10.36	9.95	4
$a_{\rm ext}$	38.76	23.53	13.73	13.61	12.71	12.19	5
	43.37	26.33	15.36	15.23	14.22	13.64	6
	7.79	4.82	2.97	2.95	2.78	2.69	4
M	6.86	4.28	2.67	2.66	2.51	2.43	5
	6.61	4.13	2.59	2.57	2.44	2.36	6

[a] In kpc.
[b] In units of 10^{11} $M_\odot$.

6. DISCUSSION AND CONCLUSIONS

Much of the total mass of our Galaxy is in a round dark halo. Of the six models considered in our calculations, the dark-halo-dominant model of Allen & Santillán (1991), model (**e**), is, in principle, the best one to estimate the Galactic mass, due to its good fit to the rotation curve and local properties. However, as shown by the results obtained with the other dark-halo-dominant simple models: (**a**) spherical, and (**c**) spherical plus disk models, the Galactic mass estimate in these sharp-boundary models is very similar, i.e., the mass estimate is sensitive to the estimated value of the escape speed v_e, but not so sensitive to the assumed form of the mass distribution. Even the very different disk model of Mestel (1963) gives a similar mass estimate. With data from our highest-velocity star W7547, these sharp-boundary models, Table 4, give a mass of $\sim 4 - 6 \times 10^{11}\ M_\odot$, and still higher $\sim 8.7 \times 10^{11}\ M_\odot$ in the sharp boundary case, $k \to \infty$, in model (**d**) (Table 5). The position of the sharp boundary is more sensitive to the assumed model, being highest ($\sim$ 125 kpc for W7547) in model (**d**).

A better model for the Galactic mass distribution would take into account a smooth density decline in the external regions, as in models (**d**) and (**f**). This modeling is very important in a mass estimate using escape speed data. A simple Galactic model of this type has been used by Kochanek (1996) in a detailed discussion of the Galactic mass. Models (**d**) and (**f**) with the external density given by eqs. (11) and (17), respectively, consider also this smooth external decline; results from these models can be compared with present estimates of the external Galactic mass (Zaritsky et al. 1989; Lin, Jones, & Klemola 1995; Kochanek 1996). The value $k = 4$ in eqs. (11) and (17) gives a similar external density decline as in the Jaffe's model used by Kochanek (1996). For model (**d**), the mass in the dark halo in the external region $a \geq a_{\rm ext}$ (eq. 11) is

$$(M_{\rm DH})_{\rm ext} = \frac{2\lambda a_{\rm ext} M_{\rm DH}((a_t)_{\rm DH})}{5\pi (a_t)_{\rm DH}} \qquad (18)$$

For the high-velocity star W7547 this mass is equal to $6.64 \times 10^{11}\ M_\odot$, $4.47 \times 10^{11}\ M_\odot$, $3.56 \times 10^{11}\ M_\odot$ for $k = 4, 5, 6$, respectively; then from Table 5, $(M_{\rm DH})_{\rm ext}/$ M is in the range $\sim 0.4 - 0.6$, and similarly in model (**f**), i.e., an important fraction of the total mass, as shown by Zaritsky et al. (1989) and Lin et al. (1995). Also, for model (**d**) there is a mass of $\sim 5 \times 10^{11}\ M_\odot$ within $a_{\rm ext}$ (Table 5), similar to Kochanek's (1996) estimate within 50 kpc. A total mass of $\sim 10^{12}\ M_\odot$, as obtained with $k = 4$, is in line with detailed estimates of Zaritsky et al. (1989), and would be of this same order in Kochanek's (1996) model. This total mass ($10^{12}\ M_\odot$) is approximately twice that of the sharp-boundary models in Table 4, for the high-velocity star W7547.

The following conclusions are in order:

1) Using our fastest stars with the lower errors, our best estimate for the lower bound to the local escape speed lies in the range 420–470 km s^{-1} in good agreement with values obtained by Sandage & Fouts (1987), Cudworth (1990), Leonard & Tremaine (1990), SPC, Kochanek (1996), and Miyamoto & Tsujimoto (1997). The stars W7547 and 811–024 have $V_{\rm T} \geq 500$ km s^{-1} and agree with the conclusion of Carney et al. (1988) that the lower bound of the local escape speed may be greater than 500 km s^{-1}; however, these two stars have $\sigma_{V_{\rm T}}$ values of ~ 100 and ~ 200 km s^{-1}, respectively, due mainly to very uncertain distances, and so do not restrict the final conclusion greatly.

2) Remarkably, for the sharp-boundary models (**a,b,c,e,** and **d** with $k \to \infty$) the mass estimate is not so sensitive to the assumed form of the mass distribution; from the simplest one-component models to the much more realistic 3-component model of Allen & Santillán (1991), the mass estimates vary by only about 25%–45%. The extended models, (**d**) and (**f**), can provide mass estimates 1.5 – 2.5 times larger, depending on the value of k.

3) For the sharp-boundary models the best lower bound to the total Galactic mass falls in the range $2.0 - 2.6 \times 10^{11}\ M_\odot$, using the stars G064–012 and HD 134439H/40H to set the lower bound to the escape speed. This is a conservative estimate since these stars have $V_{\rm T} \sim 420$–428 km s^{-1}, at the lower end of the above range, but with some of the lowest errors, $\pm$ 20–50 km s^{-1}. This mass for the Galaxy agrees well with the values estimated by Sandage & Fouts (1987), Little & Tremaine (1987), Leonard & Tremaine (1990), and SPC but is somewhat less than the estimates of Cudworth (1990; $M_{\rm TOTAL} \gtrsim 4 \times 10^{11}\ M_\odot$), Carney et al. (1988; $M_{\rm TOTAL} \gtrsim 5 \times 10^{11}\ M_\odot$) and of Kochanek (1996; $M_{\rm TOTAL} \gtrsim (4.9 \pm 1.1) \times 10^{11}\ M_\odot$) but considerably less than those of Zaritsky et al. (1989; $9.3 \pm^{4.1}_{1.2} \times 10^{11}\ M_\odot$ assuming radial satellite orbits, $12.5 \pm^{8.4}_{3.2} \times 10^{11}\ M_\odot$ assuming isotropy, and $\gtrsim 13 \times 10^{11}\ M_\odot$ from timing arguments). Little & Tremaine (1987) used Galactic satellites to measure the total mass; Zaritsky et al. (1989), satellites and Local Group timing arguments; and Kochanek (1996), all methods, as mentioned above.

4) The sharp-boundary models provide a size for the Galaxy in the range $\gtrsim$ 20–30 kpc, again using the stars G064–012 and HD 134439H/40H. However, these sizes are not compatible with the last observed point plotted on the rotation curve of Fig. 2. If a Keplerian fall-off is fit to the lower error bar of this last point, the sharp-boundary models require sizes of $\gtrsim$ 30–50 kpc, and escape speeds $\gtrsim$ 450–475 km s^{-1}, at the upper end of our estimated

range; the corresponding total Galactic mass is $\gtrsim 3.2 - 3.6 \times 10^{11}\ M_\odot$. However, this lower error bar corresponds to the radial-velocity-dispersion case of Hartwick & Sargent (1978) and of Caldwell & Ostriker (1981), from whose work this last observed point was derived. On the other hand, Sommer-Larsen, Flynn, & Christensen (1994) and Flynn, Sommer-Larsen, & Christensen (1996) have argued that the outer halo has in fact a more tangential velocity dispersion, and so the rotation curve should be fit even higher, through the last observed point of Fig. 2 or even through its upper error bar, leading to even larger sizes, escape speeds, and total masses. For comparison, Carney et al. (1988) estimated a size for the Galaxy $\gtrsim$ 40–45 kpc; Cudworth (1990), $R_{\rm limit} \gtrsim 34$ kpc; and Little & Tremaine (1987), $\lesssim 50$ kpc.

5) Our fastest star W7547 would suggest a Galactic size $\gtrsim 45$ kpc and $M_{\rm TOTAL} \gtrsim 0.5\times10^{12}\ M_\odot$ (model d) in fact gives $\gtrsim 50$ kpc and $\gtrsim 10^{12}\ M_\odot$), but with $\sigma_{V_T} \sim 100$ km s−1 this result is very tentative.

6) The rotation curves of some external galaxies extend flat to 70–80 kpc or more (Rubin et al. 1985; Rubin 1987; Sanders 1996). Freeman (1996) has argued that the rotation curve of our Galaxy extends flat out to $R \geq 100$ kpc with a value of ~ 220 km s^{-1}. If this were the case, the sharp-boundary models (a)-(c) would predict total Galactic masses $\gtrsim 0.7 - 1.1 \times 10^{12}\ M_\odot$ and would require that the local escape speed be in the range 550–580 km s^{-1}. Then, the local high-velocity stars do not define well the escape speed, falling short by 40–160 km s^{-1} and indicating that the stars are bounded or "trapped" well within escape conditions (see the discussion of Miyamoto & Tsujimoto 1997). This situation gives clues as to the formation scenario and/or environmental circumstances of the Galaxy.

7) For some of these models the contribution of the dark halo to the total galatic mass is considerable. For example, the star W7547 with the model (e) of Allen & Santillán (1991) would indicate 84% of the total mass is in the dark halo. With model (d) and the stars G064–012 and HD 134439H/40H more than 80% of the total Galactic mass is found in the dark halo, and about 50% of the total mass lies outside $a_{\rm ext}$.

The authors García-Cole, Schuster, and Parrao wish to thank extensively our coauthor E. Moreno for his considerable contribution to the undergraduate thesis of García-Cole and to the development of this publication. This work was partially supported by grants from CONACyT, Nos. 140100G202-006, D111-903865, and 1219-E9203, and DGAPA projects Nos. IN101495 and IN109596. We especially wish to thank P. E. Nissen of the University of Aarhus, Denmark, for his help and encouragement over the years! The authors are grateful to C. Allen for the loan of her computer program for calculating the space velocities and their errors. García-Cole wishes to thank Profs. R. Familiar González and J. Juárez Zúñiga for their support.

REFERENCES

Abt, H. A., & Biggs, E. S. 1972, Bibliography of Stellar Radial Velocities, Compiled at Kitt Peak National Observatory, microfiche version, Centre de Données Stellaires (Observatoire de Strasbourg)
Allen, C., & Santillán, A. 1991, RevMexAA, 22, 255
Caldwell, J. A. R., & Ostriker, J. P. 1981, ApJ, 251, 61
Carney, B. W., & Latham, D. W. 1987, AJ, 93, 116
Carney, B. W., Latham, D. W., & Laird, J. B. 1988, AJ, 96, 560
Carney, B. W., Latham, D. W., Laird, J. B., & Aguilar, L. A. 1994, AJ, 107, 2240
Cudworth, K. M. 1990, AJ, 99, 590
Eggen, O. J. 1964, Roy. Obs. Bull., No. 84
ESA 1997, The Hipparcos and Tycho Catalogues, ESA SP-1200
Fich, M., & Tremaine, S. 1991, ARA&A, 29, 409
Flynn, C., Sommer-Larsen, J., & Christensen, P. R. 1996, MNRAS, 281, 1027
Fouts, G., & Sandage, A. 1986, AJ, 91, 1189
Freeman, K. C. 1996, in IAU Symp. 169, Unsolved Problems of the Milky Way, ed. L. Blitz & P. Teuben (Dordrecht: Kluwer), 645
Giclas, H. L., Burnham, R., Jr., & Thomas, N. G. 1971, Lowell Proper Motion Survey, Northern Hemisphere, The G Numbered Stars (Flagstaff, AZ: Lowell Observatory)
_____. 1978, Southern Hemisphere Catalog, Lowell Obs. Bull., 8, 89
Hartwick, F. D. A., & Sargent W. L. W. 1978, ApJ, 221, 512
Johnson, D. R. H., & Soderblom D. R. 1987, AJ, 93, 864
Kapteyn, J. C. 1922, ApJ, 55, 302
Kochanek, C. S. 1996, ApJ, 457, 228
Leonard, P. J. T., & Tremaine, S. 1990, ApJ, 353, 486
Lin, D. N. C., Jones, B. F., & Klemola, A. R. 1995, ApJ, 439, 652
Little, B., & Tremaine, S. 1987, ApJ, 320, 493
Luyten, W. J. 1957, A Catalogue of 9867 Stars in the Southern Hemisphere with Proper Motions Exceeding 0.2″ Annually (Minneapolis, MN: The Lund Press), (LTT)
_____. 1961, A Catalogue of 7127 Stars in the Northern Hemisphere with Proper Motions Exceeding 0.2″ Annually (Minneapolis, MN: The Lund Press), (LTT)
_____. 1979, NLTT Catalogue, I, II (Minneapolis: Univ. of Minnesota)
_____. 1980, NLTT Catalogue, III (Minneapolis: Univ. of Minnesota)
Mestel, L. 1963, MNRAS, 126, 553
Miyamoto, M., & Tsujimoto, T. 1997, in Hipparcos Venice'97, ESA SP-402, 537
Nissen, P. E. 1997, private communication
Nissen, P. E., & Schuster, W. J. 1991, A&A, 251, 457 (NSV)
Nissen, P. E., Twarog, B. A., & Crawford, D. L. 1987, AJ, 93, 634
Norris, J. E., & Ryan, S. G. 1989, ApJ, 340, 739

Ochsenbein, F. 1979, 1979 Edition of SAO Stars, microfiche version, Centre de Données Stellaires (Observatoire de Strasbourg)
Pişmiş, P., & Moreno, E. 1999, in preparation
Rubin, V. C. 1987, in IAU Symp. 117, Dark Matter in the Universe, ed. J. Kormendy & G. R. Knapp (Dordrecht: Reidel), 51
Rubin, V. C., Burstein, D., Ford, W. K., Jr., & Thonnard, N. 1985, ApJ, 289, 81
Ryan, S. G., & Norris J. E. 1991, AJ, 101, 1835
Sandage, A., & Fouts, G. 1987, AJ, 93, 74
Sanders, R. H. 1996, ApJ, 473, 117
Schmidt, M. 1956, BAN, 13, 15
Schuster, W. J., & Nissen P. E. 1988, A&AS, 73, 225 (SN)
_____. 1989a, A&A, 221, 65 (SNII)
_____. 1989b, A&A, 222, 69
Schuster, W. J., Parrao, L., & Contreras-Martínez M. E. 1993, A&AS, 97, 951 (SPC)
Schuster, W. J., Parrao, L., & García-Cole, A. 1999, in progress (SPG)
Sommer-Larsen, J., Flynn, C., & Christensen, P. R. 1994, MNRAS, 271, 94
Turon, C., et al. 1992, The Hipparcos Input Catalogue (Noordwijk, The Netherlands: European Space Agency Publications Division)
Zaritsky, D., Olszewski, E.W., Schommer, R. A., Peterson, R. C., & Aaronson, M. 1989, ApJ, 345, 759

Arturo García Cole, Edmundo Moreno, and Laura Parrao: Instituto de Astronomía, UNAM, Apartado Postal 70-264, 04510 México, D. F., México (cole,edmundo,laura@astroscu.unam.mx).
William J. Schuster: Instituto de Astronomía, Observatorio Astronómico Nacional, UNAM, Apartado Postal 877, 22830 Ensenada, B. C., México (schuster@bufadora.astrosen.unam.mx.)